Kuwait J. Sci. **47 (3)** pp. 2-14, 2020

Geophysical investigation for mineral prospect in Igbeti-Moro area, southwestern Nigeria

Nurudeen K. Olasunkanmi[1*], Lukman A. Sunmonu[2], Moruffdeen A. Adabanija[2]

[1]**Physics and Materials Science Dept. Kwara State University, Malete, Nigeria.*

[2]*Pure and Applied Physics Dept. Ladoke Akintola University of Technology, Ogbomoso, Nigeria*

[2]*Earth Science Dept. Ladoke Akintola University of Technology, Ogbomoso, Nigeria*

[*]*Correspondence Author: nurudeen.olasunkanmi@kwasu.edu.ng*

Abstract

To establish significant geologic features associated with marble, gabbro, and muscovite mineralization in the Igbeti-Moro area of southwestern Nigeria, high-resolution aeromagnetic data were subjected to data enhancement processes and interpretation. The reduced-to-magnetic equator (RTE) anomaly map was subjected to various normalized (vertical, tilt and total horizontal) derivatives for lineament enhancement, edge detection of analytic signal (AS) amplitude and depth estimation techniques of source parameter imaging (SPI), averaged power spectrum and Euler deconvolution at different spectral indices. The range of RTE residual magnetic intensity from 338.3 nT to -2.4 nT (low), 9.9 to 27.7 nT (intermediate) and 32.1 to 208.0 nT (high) suggests contrasting basement lithologies in the area (viz; granite-gneiss) and the intrusion of quartz and amphibolite schists. The prominent NE – SW lineament revealed regional structural grains such as fractures and faults in these rocks associated with emplacement of the quartz-schist and muscovite-schist. This would have formed contemporaneously with isoclinal fold and host marble, gabbro, amphibolites, and muscovite mineralogy at a shallow depth range from 0 to 200 m in the western, north-central and northeastern parts of the area. The significant geologic features and their geometry of occurrences have been established as a prospect for solid minerals in the area. However, a geochemical investigation is encouraged to determine the economic value of the minerals.

Keywords: Geologic features; lineament; magnetic anomalies; mineralogy; regional structural grains.

1. Introduction

Increased demand for ornamental-stone and raw materials in industrial development and as a means of accelerating socio-economic development in Nigeria presents an opportunity to explore its areas for mineral. The deposits were mapped by the Nigeria Geological Survey Agency (NGSA) for geophysical investigation that involved a

high-resolution aeromagnetic (HRAM) survey. This was carried out between 2003 and 2009 by Fugro Survey Limited and was aimed at promoting mineral exploration in Nigeria (NGSA, 2008). However, the actual geometry of lithologic units, geologic structures, and the depth to magnetic sources of minerals can be delineated from enhanced and/or analyzed magnetic anomalies and interpretation of the resultant derivative maps such as upward and downward continuations, vertical derivative (VDR), total horizontal derivative (THDR), analytic signal, tilt (TDR) and theta derivatives vis-à-vis the geology of the area (Richard, 2001; McGraw, 2003; Moghaddam *et al*., 2015; Oladunjoye, *et al*., 2016).

Filtering and analytical tools reveal the variation in the magnetic susceptibility of the basement and that of the overlying sediments for desired improvements on the quality of the aeromagnetic data through the application of 2D Fast Fourier transform filters (Amigun *et al*., 2012). Fault block highs and a valley become obvious, and the basement structure is revealed when the enhancement and depth to magnetic sources are created by carefully analyzing a system of 2D magnetic flight lines with multiple techniques, (i.e., Source Parameter Imaging SPI, Extended Euler, Werner, Peter's Half-Slope, etc.) and then integrating data with geologic insight (John *et al*. 2003). This study aimed to establish significant geologic features as prospect for solid minerals in part of the Igbeti-Moro area of southwestern Nigeria.

2. Geological setting

The study area was located on the host state boundary between Oyo and Kwara in southwestern Nigeria. The area study had a size of about 3,064 Km2 between longitudes 4°00′ E to 4°30′ E and latitudes 8°30′ N to 9°00′ N. Its major lithological units are of the Precambrian

basement complex of southwestern Nigeria (Obaje, 2009) and comprise the older granite series, metasediments and migmatite gneiss complex (Figure 1). The basement rocks are accepted as the results of four major orogenic cycles of deformation, metamorphism, and remobilization. The cycle corresponds to the Liberian, the Eburnean, the Kibaran, and the Pan-African cycles. The extensive migmatization responsible for the Pan-African cycles was reported after the first three cycles, which have been characterized by intense deformation and isoclinal folding accompanied by regional metamorphism (Burke & Dewey, 1972). A review of geochronology work in the surrounding area by Rahaman, (1983) shows an Eburnean age (2,000 Ma) for the porphyroblastic Augen gneiss of Igbetti area. According to research in the Nigeria Geological Survey Agency Bulletin (1980), Egbuniwe reported that porphyroblastic granites are easily distinguished in East of Igbeti.

3. Materials and Methods

3.1 Data acquisition

The airborne magnetic data showed the Earth's magnetic field over Igbeti and its environ. It was measure with a Scintrex CS3 Cesium Vapor magnetometer, real-time differential GPS for the drape mode flight survey and at a sensor means terrain clearance of 75 m. Traverses were established 500 m apart with tie line spacing of 2000 m in a NE – SW direction, while flight in a NW – SE orientation was at a height of 200 m. The data points were recorded at an interval of 0.1 secs and the World Geodetic System of 1984 (WGS84) grid mesh size of 50 meters was employed. The grids were applied within UTM Zone 36S and with the Clark 1880/Arc 1960 coordinate system.

Igbeti and its environ is designated as sheet 201 of the gridded aeromagnetic data of Nigeria, after de-cultured, leveled and corrected for the international Geomagnetic Reference Field (IGRF). The grid enhanced anomaly details and reduced possible noise and latitude effects (Patterson & Reeves, 1985).

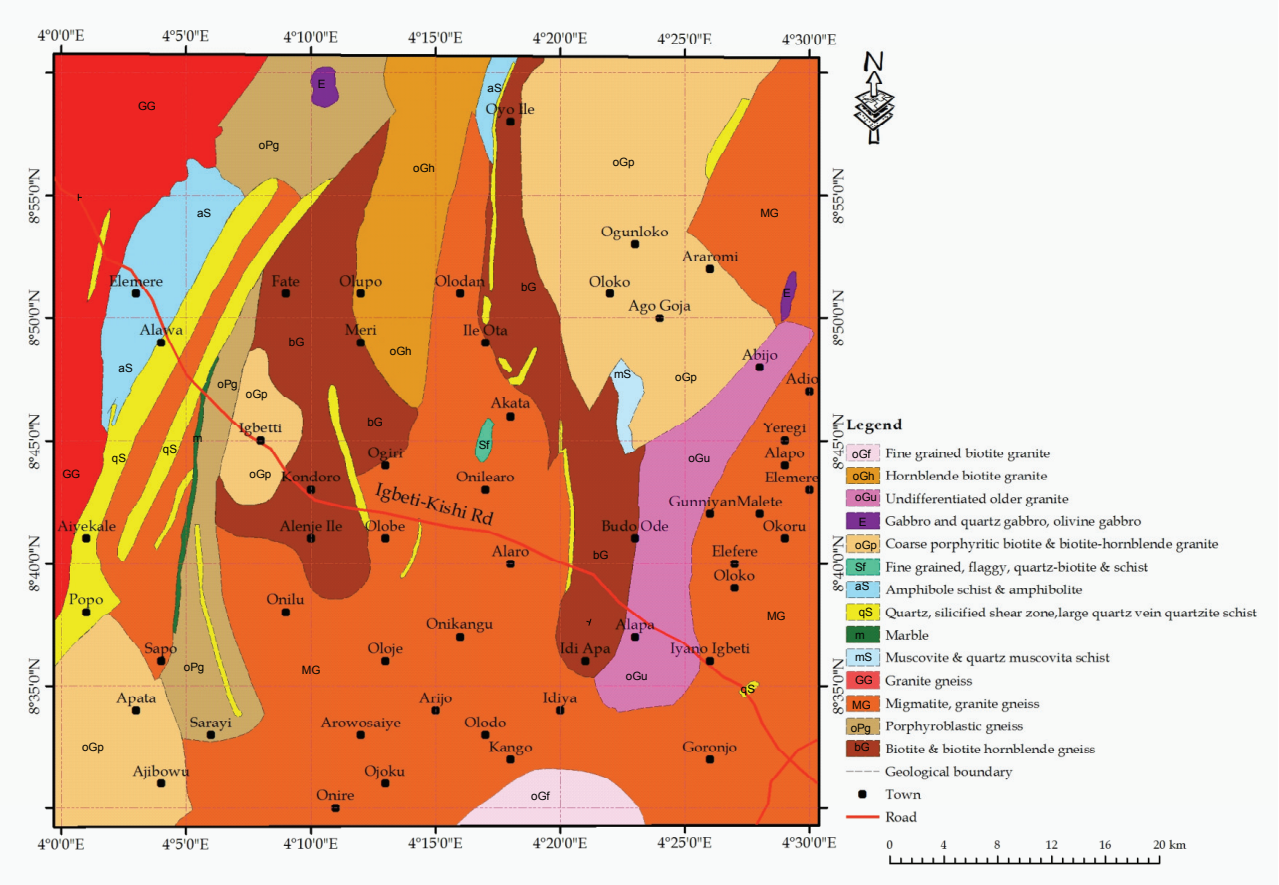

Fig. 1. Geological map of the study area (After NGSA, 2006)

The data was deployed as a total magnetic intensity field, delivered on an Oasis Montaj™ grid. It was extracted by saving the grid to a database from the grid utility tools of the program for statistical analysis (see Table 1). The minimum value was considered a static level to be reduced from each individual data value on the profiles. Anomaly maps were produced in both UTM and degrees such that the resultant derivative and analytical maps could be integrated with the geologic map of the area for a more acceptable interpretation.

3.2 Data processing and reduction

Processing and reduction of potential magnetic field data are essential tools in mineral exploration, in order to deduce meaningful interpretation (Wynn, 2002). Data processing removes both signals and spurious noise that are not related to the geologic features, thereby reducing the data to only contain signals related to the task. Aeromagnetic data processing in this study involved filtering to enhance shallow geologic features such as faults using:

1) Downward and upward continuation,

2) The conversion of data from one form to another by reducing the data to the magnetic equator (RTE) and producing the residual magnetic intensity map,

3) The detection of magnetic source body edges and lineament mapping by analytic signal amplitude ASA, vertical derivative (VDR) and total horizontal derivative (THDR),

4) Estimation of the depth to magnetic sources using source parameter imaging SPI, the average power spectrum, and Euler solution.

Table 1. Statistical analysis of the aeromagnetic data

Statistic Parameters	# of Values	Minimum	Maximum	Mean
Value	306053	37.74644	89.26064	83.39864

In some situations, source depths may be shallow and there may be major differences in degrees of magnetization, processing and reduction methods are excellent techniques(Cowan & Cooper, 2005).

The TMI data was reduced to the magnetic equator in order to correct the asymmetric and lateral shift of the measured magnetic total filed (Figure 2a). The transformation was identified to be implementable in both space and frequency domains (Aina, 1986) and is suitable for magnetic data acquired within low latitude (Baranov, 1957). The RTE residual magnetic intensity (RMI) map (Figure 2b) showed magnetic responses of rock masses or mineral deposits, their shapes, and magnitude and the direction and strength of its magnetization with respect to their global location. The upward continuation (UC) filter allowed for the modification of the measured data on one surface to some higher surface (Nabighian, *et al*., 2005) by attenuating short-wavelength anomalies relative to their long wavelength. The RTE data was upwardly continued to 200 m, 500 m, 1000 m, 2000 m, 3000 m and 4000 m (Figure 3) in order to minimize the effects of shallow sources and noise in grids (Jacobsen, 1987). The downward continuation filter enhanced the responses from data sources at a depth of 200 m by bringing the observation surface closer to the source (Trompat *et al*, 2003).

The analytic signal (/A/) is solely related to the amplitude of magnetization and is independent of the direction of magnetization. It reaches a maximum at its contact (Nabigbian, 1972). The theoretical details and mathematical models of the filters

are given in Figure 4 and Equations (1 & 2). These have been discussed by Blakely, (1995), Jacobsen, (1987) and Nabighian, *et al*., (2005).

$$|A| = \sqrt{\left|\frac{dM}{dx}\right|^2 + \left|\frac{dM}{dy}\right|^2 + \left|\frac{dM}{dz}\right|^2}. \quad (1)$$

$$Tilt\ derivative\ (\theta) = \tan^{-1}\left(\frac{VDR}{THDR}\right). \quad (2)$$

The rate of change of the magnetic field spatially in vertical and horizontal directions is quantified with vertical and horizontal derivatives (Ross, 2002). The vertical derivative (VDR) of the observed potential fields is explained as a measure of the change in gradient. The first VDR was used in this study to increase the clarity of local anomalies obscured by broader regional trends. It aided in the edge detection of source bodies. Cooper and Cowan (2004) observed that small-size mineralized bodies stand out more conspicuously with the use of VDR

as its plotted values have the effect to make potential field from the local features. An increase in the order derivative -a form of the high-pass filter- increases the pronounced effect and enhances the noise in the data in a similar way. The first vertical derivative map (Figure 5a) exaggerated shallow features. It also leveled the differences between the survey lines. However, the THDR (Figure 5b) and ASA (Figure 6) delineate limits of intrusive bodies, faults, and other lateral changes (see Figure 7).

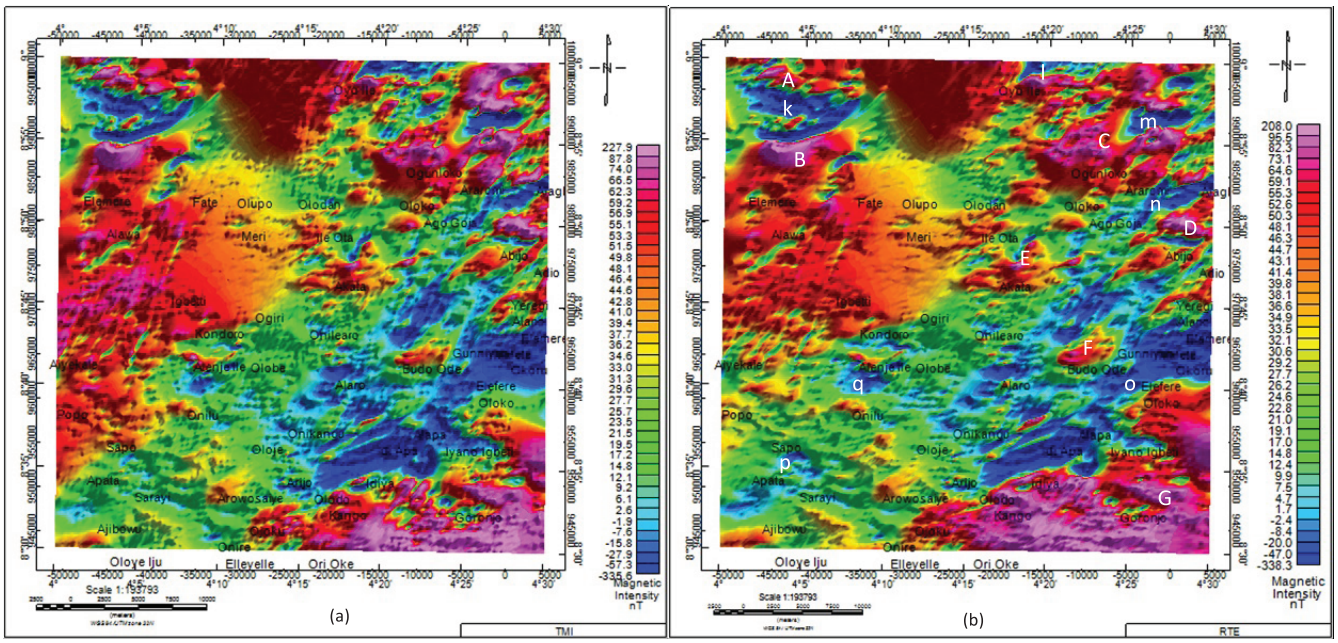

Fig. 2. Comparison of (a) the total magnetic intensity and (b) the Reduced to Equator Residual Magnetic Intensity maps

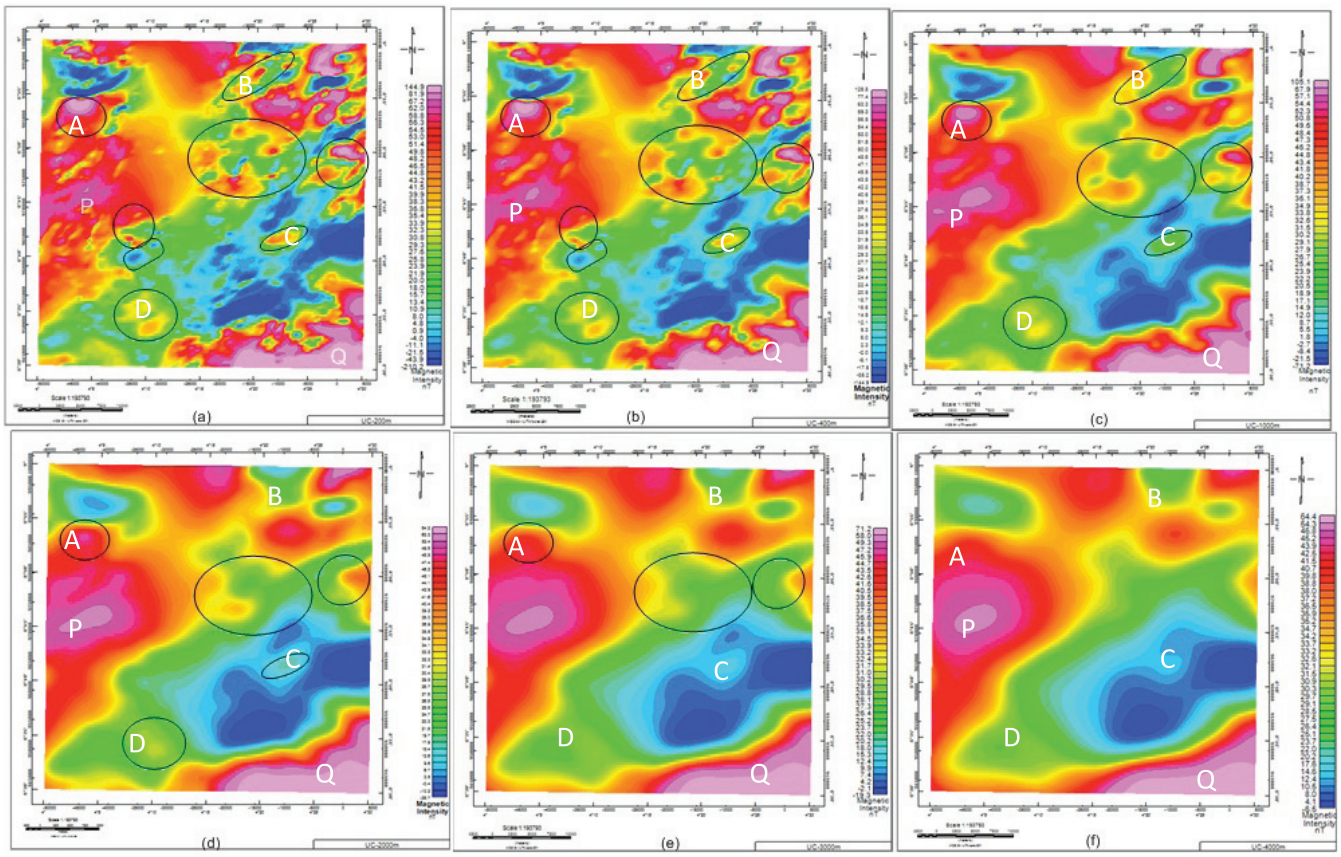

Fig. 3. Magnetic amplitude map obtained from RTE residual aeromagnetic intensity map after upward continuation; (a) to 200 m; (b) to 400 m; (c) to 1000 m; (d) to 2000 m; (e) to 3000 m and; (f) to 4000

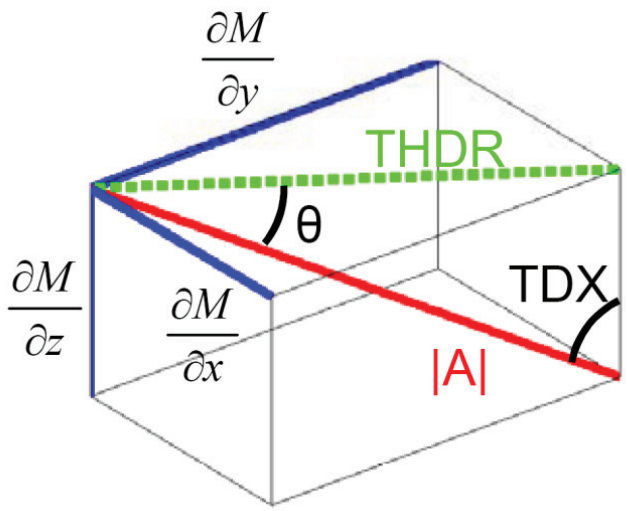

Fig. 4. Relationship between total horizontal derivative (THDR), analytical signal amplitude (|A|) and tilt angle (θ) by Fairhead & Williams (2006), adopted from Paananen (2013)

The maximum magnitude of the horizontal magnetic gradient anomaly occur above geological boundaries such as faults or steeply dipping lithological boundaries. Areas of steep lateral gradient have higher scalar amplitude values of the horizontal magnetic gradient (Blakey & Simpson, 1986).

There are different depth estimation tools that researchers can employ depending on the data required. Depth can be divided into three ranges as presented in Table 2. For best results with some tools, they are configured according to the depth of the sources of interest. The SPI method (Thurston *et al*., 1999) estimated from the local wavenumber of the analytic signal, the depth to magnetic source and its accuracy was ± 20% in tests on real data sets with drill-hole control. The power spectrum method has been especially useful in determining the average depth to an ensemble of magnetic sources observed on maps (Spector & Grant, 1970; Robinson & Treitel, 2000). Spectral analysis shows magnetic field anomalies with trends approaching a natural power-law spectrum such that a lot of energy comes from large, deep sources (at low wavenumbers). Relatively little energy (orders of less magnitude) from small, shallow ones (high wavenumbers) with an approximately exponential decay with wavenumber (Reeves, 2005). The Euler Deconvolution technique uses first order x, y, and z derivatives to determine location and depth for various idealized targets (sphere, cylinder, thin dyke, contact). Each is characterized by a specific structural index (Table 3). This study utilized the SPI on the Oasis montaj's submenu tool for an automatic location and depth determination of causative bodies from gridded magnetic data, the average depth estimate from the power spectrum, and a Euler solution for geometry and possible mode of occurrence of geologic formation at depths.

4. Results and Discussion

Comparing the RTE map with the total magnetic intensity map (Figure 2) shows no significant modification of the original magnetic anomalies marked as positive and negative anomalies A, B, C, D, E, F, G, and k, l, m, n, o, p, q, r, respectively. The amplitude of the anomalies range from – 338.3 nT to 208.0 nT. These outcome were consistent in the pattern, trend, and amplitude of the original magnetic anomalies which fall within – 335.6 nT to 227.7 nT. This shows that the data has been well filtered. The southeast and northwestern regions of the RTE map are characterized by positive (high) magnetic intensity value range between 32.1 nT to 208.0 nT, The west and north – northcentral regions host an intermediate magnetic value range from 9.9 to 27.7 nT, while the northeast to east, central and southwestern regions have a negative anomaly range between - 338.3 nT to - 2.4 nT. However, varying amplitude (decreasing/stable/increasing) of the magnetic anomalies at greater upward continuations were revealed.

Table 2. Depth ranges of interest described by Intrepid, (2012)

Depth Interval	Explanation	Interest
200 m–0	Shallow	Mineral exploration, Environmental studies, Water resources
1000 m–200	Intermediate	Mineral exploration, Water resources
Deeper than 1000 m	Deep	Oil exploration, Mineral exploration

Table 3. Structural indices for various geological models (*SI*: Thompson, 1982).

Geological Model	Number of Infinite dimensions	Magnetic SI
Sphere	0	3
Pipe	1 (Z)	2
Horizontal cylinder	1 (X or Y)	2
Dyke	2 (Z and X or Y)	1
Sill	2 (X and Y)	1
Contact	3 (X, Y and Z)	0

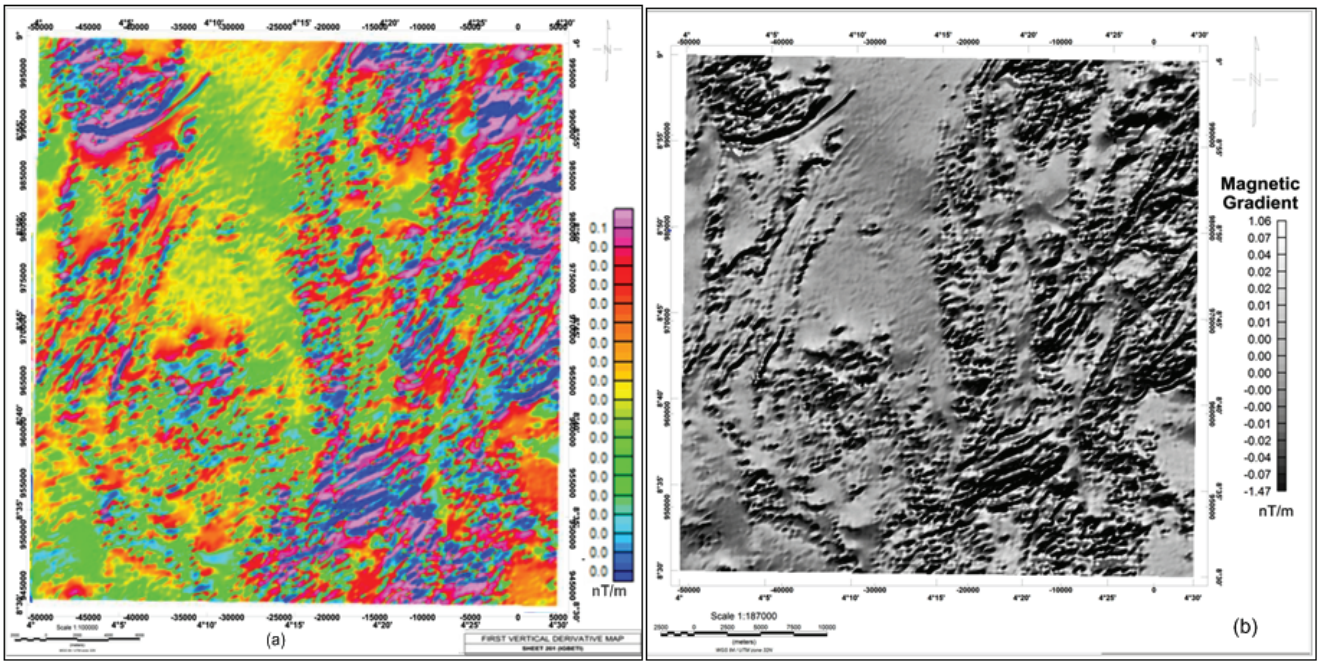

Fig. 5. (a) Vertical and (b) total horizontal Derivative maps

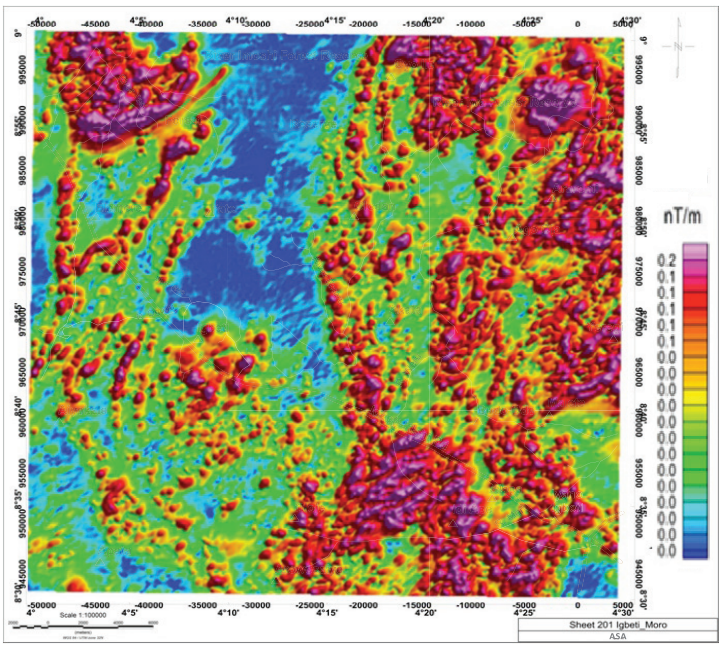

Fig. 6. Analytic Signal Amplitude map

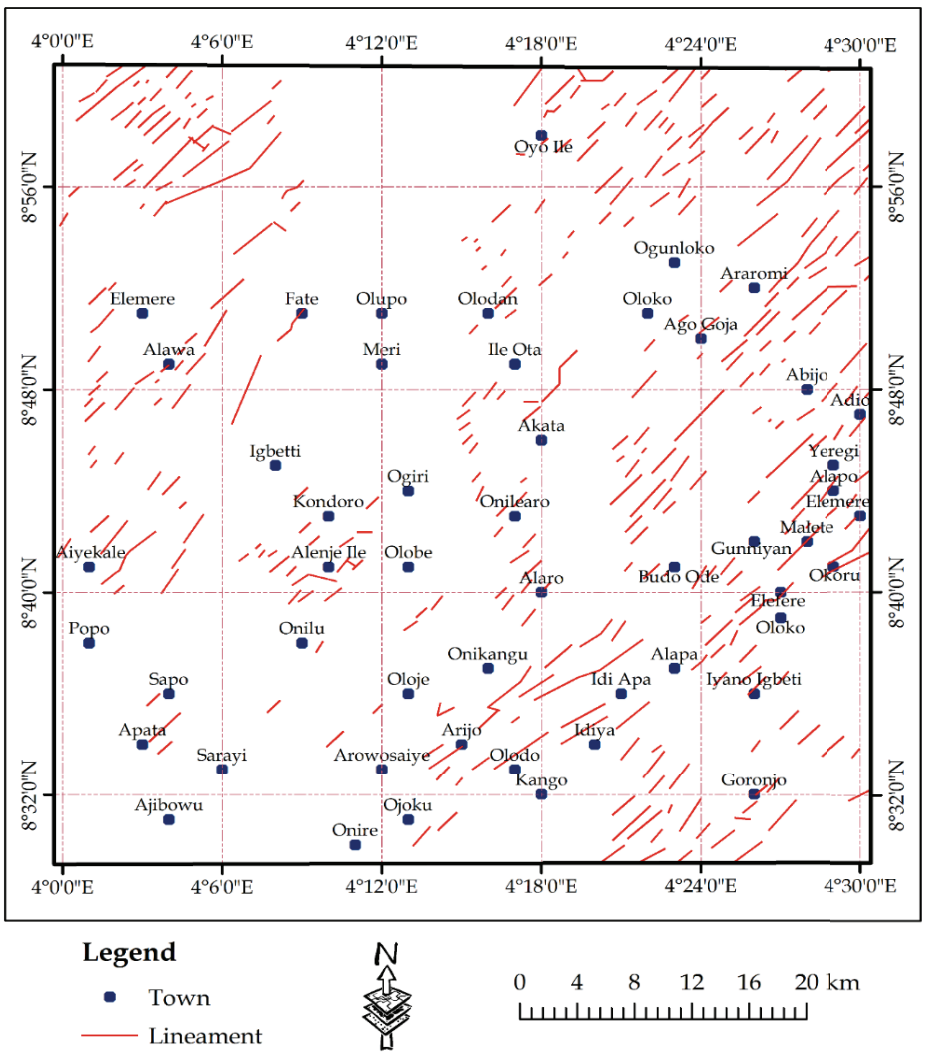

Fig. 7: Lineament extracted from the derivative maps of RTE anomaly map of Igbeti

Relatively high positive magnetic anomalies are depicted by P and Q in Figure 3. They have an intensity range from 46.8 to 121.1 nT in the eastern and southwestern regions, respectively. The anomalies are visible at an upward continuation distance of 200 m and retains the same magnitude with increasing upward continuation to 4000 m. This accentuates the depths of 100 m and 2000 m, respectively, in concordance with the rule of thumb, "data depth-continued at a height of z corresponds to the depth of of z/2" (Paananen, 2013).

The regions delineated by a black ellipse at the northeastern, central, eastern, northwestern and southwestern part experienced an abrupt change in amplitude (from high to low) and are considered fault zones in concordance with Paananen (2013) and Oladunjoye *et al*, (2016) fault identification. The ASA map (Figure 6) showed the magnetic zone with high amplitude of 0.061 - 0.53 nT/m (pink), prominent in the northwest, northeast to the east and southeastern regions. However, regions with a low amplitude range ≤ 0.00 to 0.004 nT/m (blue) are visible in the north central to west, southwest and extreme southeast. There is a conspicuous intermediate magnetic amplitude within 0.006 to 0.060 nT/m (green to red).

4.1 Basement Mapping

Careful examination of the RTE map (Figure 2b) with the geological map (Figure 1) showed that the alternating positive and negative magnetic values suggest a rock contrast in the basement of the study area. The intermediate magnetic anomalies are connected with the intrusion of quartz and amphibolite schists bounded by relatively low magnetic intensity which is associated with older granitoid (Biyiha-Kelaba *et al*., 2013). The negative anomalies are related to mining and prospecting areas (Hanna, 1969) of marble, gabbro, amphibolites and muscovite mineralogy within the granite-gneisses in the west and north – northcentral regions. These areas commonly carry small amounts of magnetite and dark minerals like biotite and hornblende (paramagnetic). The minerals could have been deposited in the quartz vein (Hans, 2012) or have resulted from the intrusion of hydrothermal fluids which can deposit less magnetic materials in fractured rock (Jayeoba & Odumade, 2015). The positive magnetic anomaly amplitude is allied with gneiss complex rocks namely; granite gneiss, migmatite gneiss and biotite gneiss, all which make up the various lithologic units in the area (Telford *et al*., 1990; Oladunjoye, 2016).

4.2 Depth to basement estimate

Figure 8a shows the computed amplitude spectrum again wave-number on a logarithm scale from the Fourier transformation for the aeromagnetic data. The depth curve in the figure has a straight line segmented into three with increasing frequency as the slope decreases. The red line (first) segment has a gradient of about – 3.67, the green line (second) has a gradient of about - 0.67, and blue line (third) segment has a gradient of about - 0.25. The peaks within the lowest gradient give the depth estimate of the shallow source as 100 – 220 m while the peaks in the greatest descent give the depth estimate of the deepest source as 190 m – 740 m. The SPI (Figure 8b) compliment the depth estimate for a shallow to deeper basement source range of - 335.6 m to 227.9 m while the Euler solutions (at SI = 0, 1, 2) revealed distinct clustering around a tadpole-like and south-north trending marble in the west, gabbro in the east and north, as well along lineaments associated with the quartz and muscovite schist (Figure 9). There was an estimated depth range of less than zero to above 300 m (shallow mineral exploration depth range classification of Intrepid, 2012). These solutions correspond to a contact, sill/dyke and horizontal cylinder geological model of the causative bodies (Reid *et al*., 1990; GETECH, 2007; Olasehinde *et al*., 2012). Conversely, the result of the Euler solution obtained at SI = 3.0 (Figure 9d) shows no notable clustering around some geologic structures nor around some magnetic anomalies. Hence, they are not considerable solution and are rejected in concordance with the Euler solution classification of Thompson (1982), Reid *et al*. (1990) and Feumoe *et al*. (2012).

4.3 Structural framework

On the premise that some geologic structures or sedimentary features, such as faults or channels, host magnetic minerals which are mostly concentrated along or aligned with the lineaments, the total horizontal derivative map of the area has been interpreted to infer the prominent geological structures associated with the lineaments. The lineaments were superimposed on RTE magnetic intensity map (Figure 10a) using Arc-GIS 10.3 software. They are characterized geologically as either ductile or brittle when their orientation is concordant or discordant with magnetic anomalies (Paananen, 2013). The scanty east-west lineaments are in concordance with the east-west magnetic anomalies enclosed in a black oval. They indicate a ductile deformation, while the areas dominated by NE - SW and a few NW – SE lineaments are brittle deformation zones. The ductile could exhibit structural features such as faults and fractures. The

magnetic fault characterization map was obtained by superimposing the lineaments on the geological map (Figure 10b). The faults are represented in green and red and interpreted as sinistral and dextral, respectively due to their different orientations: N–S, E–W, WWS – EEN, SSW – NNE, and WWN – EES. The sinistral faults indicate the emplacement of quartz-schist and muscovite-schist, which host the marble, gabbro, amphibolites and muscovite mineralogy prior to deformation. This has led to the formation of sinistral faults observed at the eastern, western and north-central parts of the study area. There is a dominantly low analytic signal amplitude in the N-NW and sparingly in the S-SW areas (Fig. 5). This means that the host rock is more magnetic than the intrusive rocks. This could result from extreme topography, reversed remanent magnetization (Hans, 2012), or it could be associated with weakly magnetic rock which have been polarized t a contact with more highly magnetic rocks (Hanna, 1969). (See the pink are of Figure 5).

5. Conclusions

High-resolution aeromagnetic data of Igbeti-Moro was processed, enhanced and analyzed using Oasis Montaj geo-software in order to map geologic structures associated with mineral exploration in the area. The interpretation of filtered magnetic anomalies and resultant derivative maps indicated marble, gabbro, amphibolites and muscovite mineralogy within veins and sheared rocks in western, northern and northeastern parts of the area. These are bounded by gneiss and older granitoid. The minerals exist at a shallow depth range from 0 – 200 m and may have possibly been deposited by the intrusion of hydrothermal fluids along quartz schist veins during the block rotation of identified sinistral and dextral faults. The pattern of occurrence and associated geologic structures suggests that the minerals are structurally controlled, which is critical in mining operations.

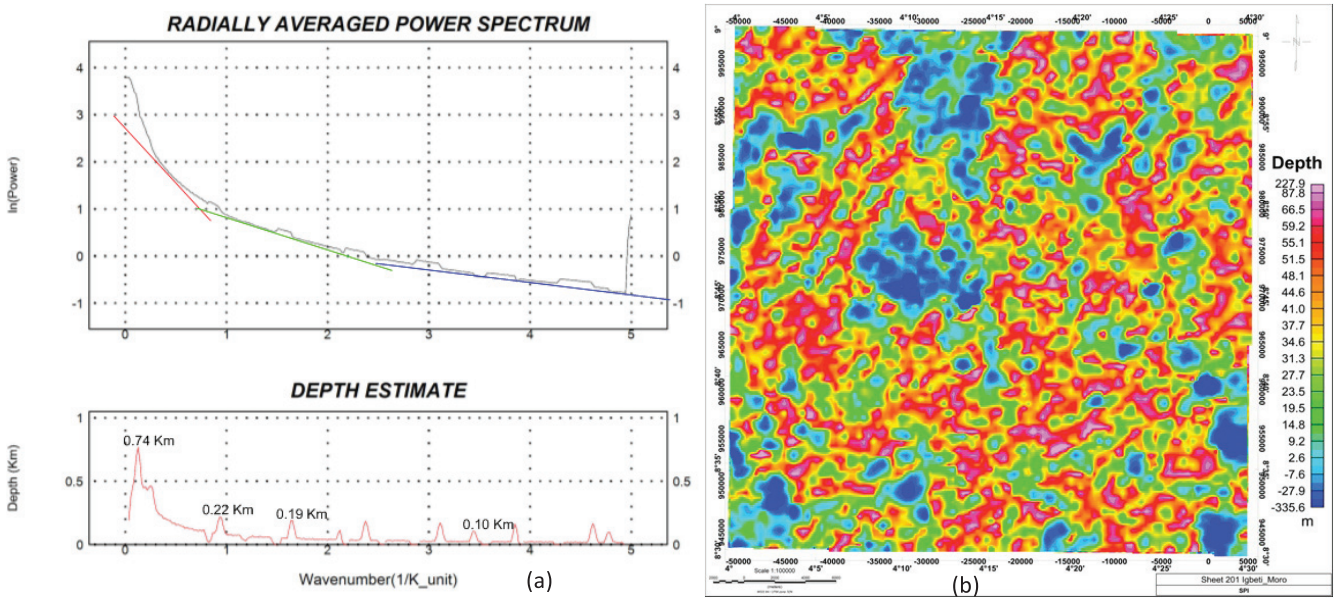

Fig. 8 (a) Radially averaged power spectrum depth and (b) Source Parameter Imaging depth estimate maps

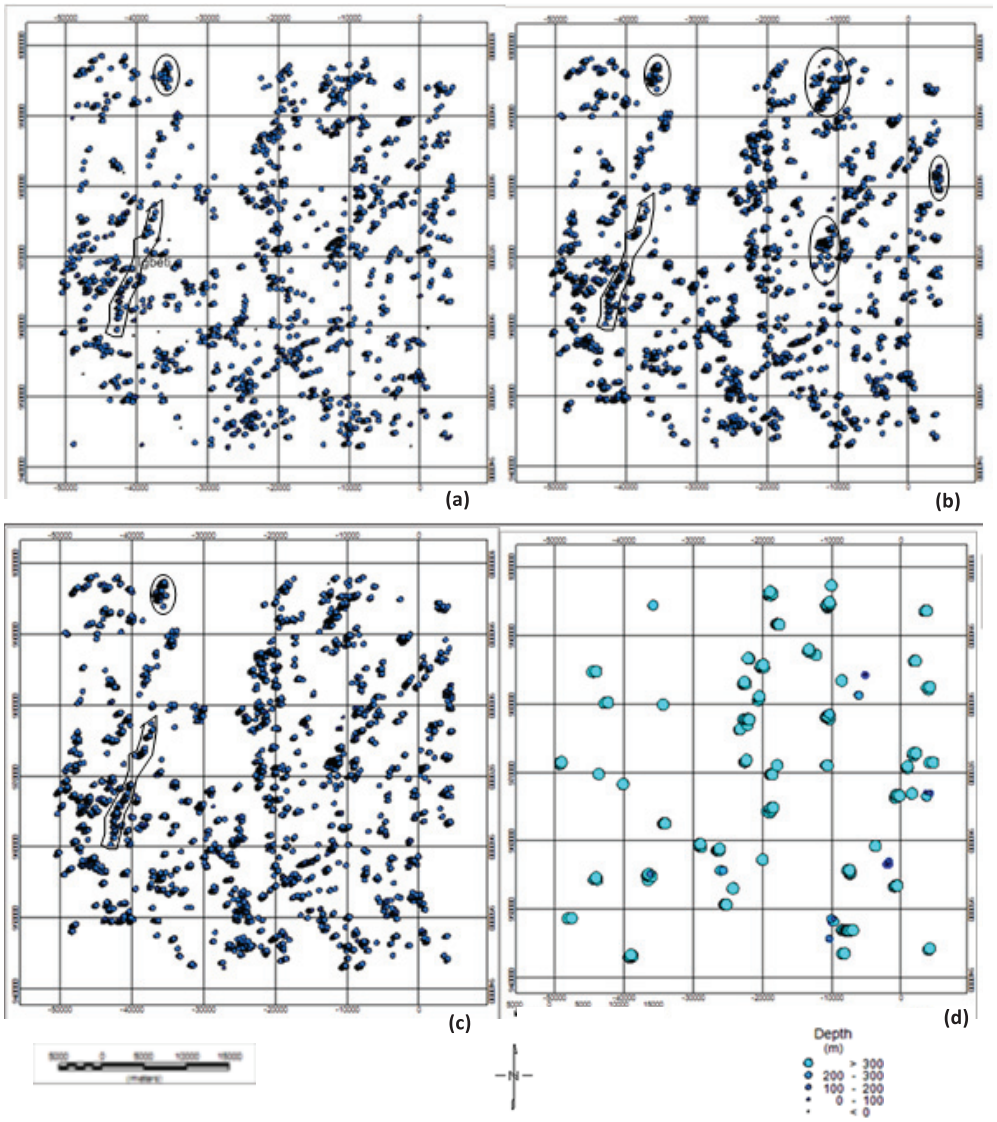

Fig.9: Euler deconvolution depth estimate from the RTE residual anomalies at (a) SI = 0, (b) SI = 1, (c) SI = 2 (d) SI = 3

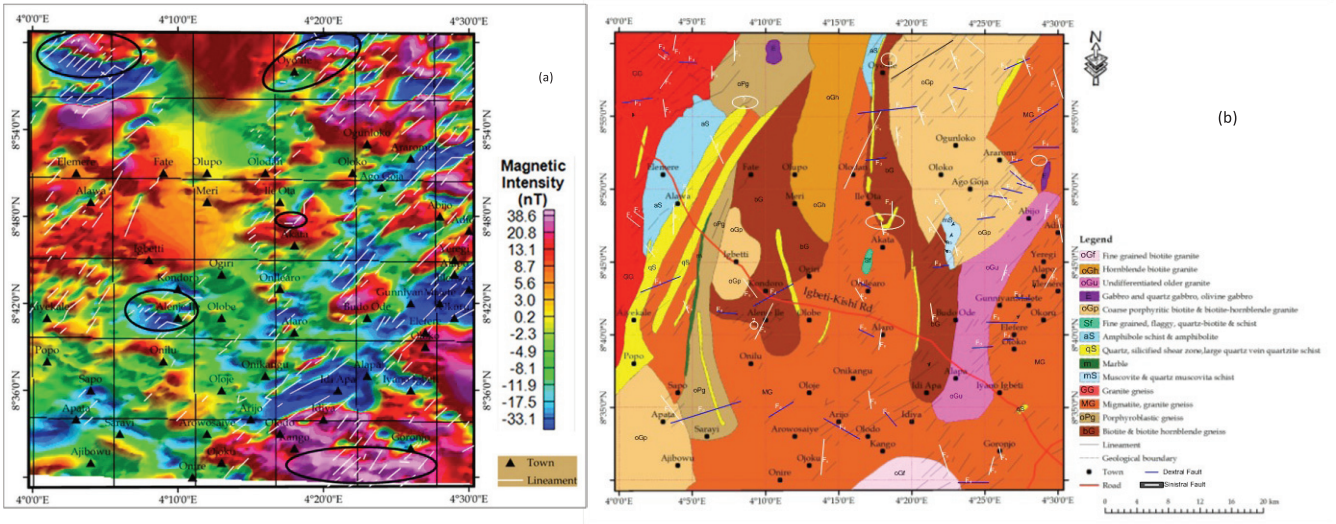

Fig. 10 Fault classification maps showing the extracted lineaments from THDR overlaid on (a) RTE magnetic intensity and (b) geological maps

References

Amigun, J. O., Afolabi, O., & Ako, B. D. (2012). Application of airborne magnetic data to mineral exploration in the Okene iron ore province of Nigeria. International Research Journal of Geology and Mining (IRJGM), 132-140.

Baranov, V. (1957). A new method for interpretation of aeromagnetic maps, pseudo-gravimetric anomalies. Geophysics, **22**: 359 - 383.

Blakely, R. J. (1995). Potential theory in gravity and magnetic applications. Cambridge University Press. New York, 435.

Blakely, R. J., & Simpson, R. W. (1986). Locating edges of source bodies from magnetic and gravity anomalies. Geophysics, **51**(7): 1494 - 1498.

Biyiha-Kelaba, W., Ndougsa-Mbarga, T., Yene-Atangana, J., Ngoumou, P. C., & Tabod, T. C. (2013). 2.5D Models derived from the magnetic anomalies obtained by upwards continuation in the Mimbi area, southern Cameroon. Journal of Earth Sciences and Geothecnical Engineering, **3**(4): 175-199.

Burke, K. C., & Dewey, J. F. (1972). Orogeny in Africa. Dessauvagie, T F & Whiteman, A J. Africa geology, University of Ibadan Press, Ibadan, 583–608.

Cooper, G. R., & Cowan, D. R. (2004)

Filtering using variable order vertical derivatives. Computers & Geosciences, **30:** 455-459.

Cowan, D.R., and Cooper, G.R.J., (2005), Enhancement of magnetic signatures of impact structures. Kenkmann, T., Hörz, F., and Deutsch, A. Large meteorite impacts III. Geological Society of America special paper 384: 51–65.

Egbuniwe, I. G., (1980). The geology of part of southwestern Nigeria, Geological Survey of Nigeria Bulletin, **31**(26): 1-47.

Fairhead, J. D., & Williams, S. E. (2006) Evaluating normalized magnetic derivatives for structural mapping. SEG annual meeting New Orleans, Louisiana.

Hanna, W. F. (1969). Negative aeromagnetic anomalies over mineralized areas of the boulder batholith, Montana. Geological survey professional paper, 650: D155–D167.

Hans, T. (2012). Magnetic survey at

Nesodden - survey and interpretation report. Lulea: GeoVista AB.

Intrepid, (2012). Estimating source depth-overview (C01). Intrepid Geophysics, Brighton Australia.

Jayeoba, A., & Odumade, D. (2015). Geological and structural interpretation of Ado-Ekiti southwest and its adjoining areas using aeromagnetic data. Pacific section AAPG, SEG and SEPM joint technical conference. Oxnard, California USA.

Jacobsen, B. H. (1987). A case for upward continuation a sa standard seperation filter for potential field maps. Geophysics, 1138 – 1148.

John, M. J., Marianne, E. P., & Antony, D. P. (2003). Improving geologic understanding with gravity and magnetic data: Examples from Gabon, Nigeria and the Gulf of Mexico. EAGE, 57-62.

McGraw, H. (2003). Dictionary of geology and mineralogy (2nd ed.). United State of America McGraw-Hill Companies.

Moghaddam, M., Mohammad, S., Saeid, M., & Nasim, H. (2015). Interpretation of aeromagnetic data to locate buried faults in north of Zanjan Pprovince, Iran. J Remote Sensing & GIS, **4**(2): 1 - 5.

Nabighian, M. N. (1972). The analytic signal of two-dimensional magnetic bodies with polygonal cross-section: its properties and use for automated anomaly interpretation. Geophysics, 507-517.

Nabighian, M. N., Grauch, J. S., Hansen, R. O., LaFehr, T. R., Li, Y., *et al* (2005). The historical development of the magnetic method in exploration. Geophysics, 33 - 61.

Nigerian Geological Survey Agency, (2008). Airborne Geophysical Survey: total magnetic intensity of Igbeti (Sheet 201).

Nigerian Geological Survey Agency, (2006). Geological map of Igbeti (Sheet 201) Area.

Obaje, N. G. (2009). Geology and mineral resources of Nigeria. Lecture Notes in Earth Sciences. Berlin Heidelberg: Springer.

Oladunjoye, M. A., Olayinka, A. I., Alaba, M., & Adabanija, M. A. (2016). Interpretation of high resolution aeromagnetic data for lineaments study and occurence of banded iron formation in Ogbomoso area, Southwestern Nigeria. Journal of African Earth Sciences, 43-53.

Paananen, M. (2013). Complete lineament interpretation of the Oikiluoto region. Posiva, 2013-02 ISBN 978-951-652-234-3.

Rahaman, M.A., Emofurieta, W.O. Vanchette, M.C., (1983) The potassic granites of Igbetti Area: further evidence of the polycyclic evolution of the Pan-African Belt in SW Nigeria. Precambrian Research, **22**(1-2): 75-92.

Reeves, C. (2005). Aeromagnetic Surveys: principles, practice and interpretation. Geosoft.

Richard, A. M. (2001). Dictionary of geophysics, astrophysics and astronomy. CRC Press, Boca Raton London New York Washington, D.C.

Robinson, E. A., & Treitel, S. (2000). Geophysical signal analysis. Tulsa, USA: Society of Exploration Geophysics.

Ross, C. B. (2002). Geophysical and remote sensing methods for regolith exploration. Geoscience, Australia.

Telford, W. M., Geldart, L. P., Sheriff, R. E., & Keys, D. A. (1990). Applied geophysics. Cambridge University Press.

Thurston, J. B., Guillon, J. C., & Smith, R. S. (1999). Model independent depth estimation with the SPITM method. 69th Annual international meeting. Society of Exploration Geophysics. 403– 406.

Trompat, H., Boschetti, F., & Hornby, P. (2003). Improved downward continuation of potential field data. Exploration Geophysics, 249 - 256.

Spector, A., & Grant, F. S. (1970). Statistical models for interpreting aeromagnetic data. Geophysics, 293 - 302.

Wynn, J. (2002). Evaluating ground water in arid lands using airborne magnetic and airborne electromagnetic methods- and example in the southwestern U.S. and northern Mexico. The L62 -65.

Submitted: 09/04/2018
Revised: 30/10/2018
Accepted: 11/11/2018

جيوفيزيائية للنقيب عن المعادن في منطقة Igbeti-Moro ايجيبتي–مورو بجنوب غرب نيجيريا

نوردين ك. أولاسنكانمي، لوكمان ا. سنمونو، مورفدين ا. ادابنيجا
قسم الفيزياء وعلوم المواد، جامعة Kwara،ماليت Malete، نيجيريا

الملخص

يهدف البحث لدراسة الخواص الجيولوجية المهمة المرتبطة بتعدين الرخام وصخور الجابرو ومعدن المسكوفيت في منطقة ايجيبتي–مورو في جنوب غرب نيجيريا، ولتحقيق ذلك تخضع بيانات المغناطيسية الجوية عالية الدقة للتفسير وعمليات تعزيز البيانات. كما تم اخضاع (RTE) الخريطة الشاذة المُصَغرة لخط الاستواء المغناطيسي لعدة مشتقات طبيعية متنوعة (عمودية، مائلة، أفقية بالكامل) بغية تعزيز التخطط، والكشف الحدى للمؤشر التحليلي (AS) لعُمق وسعة آليات تقدير مُعامل المصدر (SPI)، وطيف الطاقة المتوسطة وإزالة الالتفاف اليولري وفقاً لفهارس طيفية مختلفة. كما يشير وجود نطاق من RTE تتراوح فيه شدة المغناطيسية المتبقية من 338.3 nT إلى 2.4– nT (منخفض) ومن 9.9 إلى 27.7 nT (متوسط) ومن 32.1 على 280.0 nT (عالي) لوجود قواعد ليثولوجية متناقضة في المنطقة (بمعنى، أصل الجرانيت) وتدخل الكوارتز وشست الأمفيبوليت. كما يكشف الميل الشمالي الشرقي– الجنوبى الغربي حبيبات بنيوية إقليمية (مثل الصدوع والشقوق) في تلك الصخور والمرتبطة بوضع شست – الكوارتز وشست المسكوفيت اللذان تكونا بالتزامن مع طية متفقة الميل، كما تتضمن علم المعادن الخاص بالرخام والجابرو والأمفيبوليت والمسكوفيت الموجودة على أعماق ضحلة تتراوح بين 0 إلى 200 متر في الأجزاء الغربية، والشمالية الوسطى والشمالية الشرقية من المنطقة. وقد اتُخذت الخواص الجيولوجية المهمة وهندسة البروزات الخاصة بها كأساس للتنقيب عن المعادن الصلبة في المنطقة. ومع ذلك يتم تشجيع البحث الجيوكيميائي لتحديد القيمة الاقتصادية للمعادن.